# Tuesday Evening Poster Sessions, October 22, 2019

## Surface Science Division
## Room Union Station AB - Session SS-TuP

### Surface Science Poster Session

**SS-TuP-1 Mechanistic Studies of Thermal Dry Etching of Cobalt and Iron Thin Films**, *Mahsa Konh, A Teplyakov,* University of Delaware

Thermal dry etching of cobalt and iron thin films were investigated using diketones. Two diketones (1,1,1,5,5,5-hexafluoro-2,4- pentanedione (hfacH) and 2,4-pentanedione (acacH)) were used to show their reactivity toward cobalt and iron thin films with the results being relevant to etching of CoFe alloys. To understand the mechanism of etching process, possible surface reaction pathways were followed with temperature programmed desorption (TPD). Resulting surfaces were characterized using X-ray photoelectron spectroscopy (XPS) supplemented with microscopic investigations. Starting with oxidized or halogenated surfaces was found to be necessary to form volatile products that would make etching possible. However, halogenation makes the mechanism more complicated. It was shown that several products were desorbing from the halogenated metal surfaces containing $M^{2+}$ and $M^{3+}$. These products may also contain both the organic ligands and halogens. The effect of dosing temperature on the etching process was also investigated.

**SS-TuP-2 Reaction of ZnO Nanomaterial with a Mixture of Gas-phase Prop-2-ynoic acid and Acetic Acid to Control Surface Coverage of Reactive Functional Groups**, *Dhamelyz Silva-Quinones, A Teplyakov,* University of Delaware

Sensitization of oxide nanomaterials with a two-step process involving the reaction with gas-phase prop-2-ynoic acid followed by "click" attachment of functionalized azides to the resulting alkyne functionality has been recently reported by our group. One advantage of the first modification step being a gas phase reaction with a nanomaterial is in the ability to control surface concentration of alkyne functionality by dosing predetermined mixtures of prop-2-ynoic acid with another compound (in this case acetic acid) that reacts with the oxide surface in exactly the same way as prop-2-ynoic acid but does not lead to the formation of a reactive functionality to be utilized in the second step of sensitization. This approach is demonstrated for the mixture of these acids reacting with ZnO nanomaterial, and the concentration of surface alkyne functional groups is determined by the concentration of the prop-2-ynoic acid in the mixture with acetic acid. The resulting functionalized surface is interrogated by infrared spectroscopy to demonstrate that both acids co-adsorb on ZnO. Vibrational signatures of the $CH_3$ group at 1453 $cm^{-1}$ and that of the alkyne group at 2110 $cm^{-1}$ allow for quantification of the co-adsorbed species. This assessment is confirmed by the XPS investigation utilizing different ratios of the C 1s features corresponding to carboxylates compared to the methyl/alkyne carbon atoms in mixtures of pro-2ynoic and acetic acids. Solid state NMR spectroscopy is used to further confirm the formation and to quantify the concentration of two components in the mixed monolayer.

**SS-TuP-3 Platinum Deposition onto OH-terminated Si (100) and Boron-impregnated Si (100) Substrates**, *Sana Rani, C Byron, A Teplyakov,* University of Delaware

Trimethyl(methylcyclopentadienyl)platinum(IV) was used as a precursor to deposit platinum on silicon surfaces using wet chemistry method. The deposition was performed on silicon based substrates including oxidized (OH-terminated) Si(100) and boron-impregnated oxidized Si(100) surface. Fourier-transform infrared spectroscopy (FTIR) was used to confirm the purity of the precursor. The deposition process was performed at room temperature after activation of substrates at 200°C. The successful deposition resulted in formation of nanoparticles as confirmed by atomic force microscopy (AFM) with $PtO_x$ being the majority deposited species as confirmed by X-ray photoelectron spectroscopy (XPS). These substrates were later calcined at 400°C followed by an activation at 550°C under $H_2$ gas environment. This activation procedure resulted in a reduction process that led the formation of metallic Pt particles as confirmed by XPS. The reactivity of precursor and dispersion of Pt nanoparticles on OH-terminated Si(100) surface was compared to that of B-impregnated surface. Calcination and activation under high temperature resulted in highly dispersed Pt nanoparticles on B-impregnated substrates.

**SS-TuP-4 Barium Adsorption and De-wetting on W(112)**, *Michael Mroz,* Ohio University; *S Tenney, C Eads,* Brookhaven National Laboratory; *M Kordesch,* Ohio University

The tungsten (112) surface has been observed with adsorbed barium in emission microscopy. The barium metal is deposited from a filament filled with a piece of metallic barium. When the barium layer on the W(112) surface is heated, the barium de-wets, forming a "wetting layer" and droplets of barium. The de-wetting is solid-solid de-wetting, because the rupture of the film into droplets occurs at about 1/3 of the barium melting temperature (727 C). At low coverage, about 20 nm barium, the droplets are sparse, and the wetting layer uses most of the available barium. Two 2x1 domains and weak centered 2x2 low energy electron diffraction (LEED) pattern are observed. At high coverage, about 200 nm, in addition to the wetting layer, and a dense coverage of droplets ( 250 nm diameter), there are also larger scale networks of barium drops spread over micron scale distances.

**SS-TuP-5 Self-Catalyzed Gas-Phase Cycloaddition on "Clickable" Nanostructured CuO Surface**, *Chuan He, A Teplyakov,* University of Delaware

The surface functionalization of nanostructured metal oxides (CuO, ZnO, $TiO_2$, $CeO_2$) has attracted substantial attention due to their extensive applications in sensing, photo-catalysis, electronics, and energy conversion. A number of studies have been reported to achieve the surface sensitization of these metal oxides with organic or organometallic compounds in order to expand their versatile properties by introducing designated functionality. However, the most common approach to achieve this functionality utilizes sensitizer molecules reacting with oxide surfaces via carboxylic (COOH) or phosphonic $(P(O)(OH)_2)$ anchor groups or by silylation (such as with $R-Si(X)_3$, where the X could be Cl or $-OCH_3$), which potentially leads to agglomeration, multilayer growth, or surface etching. Our recent research developed a two-step functionalization approach utilizing exposure of the oxide materials to prop-2-ynoic acid (HC≡C-COOH, prop-2-ynoic acid) in the gas phase as a first step, followed by second step of post-modification exploiting the created C≡C to introduce any pre-designed functionality to the surface via Cu(I)-catalyzed "click" chemistry with azides ($R-N_3$). More importantly, this approach requires no additional presence of the copper catalyst for nanostructured CuO due to the reduction of surface copper from prop-2-ynoic acid modification. As a result, the second step of this functionalization can be achieved through self-catalyzed cycloaddition with gas-phase species. The morphology preservation and selective covalent attachment of the carboxylic acid onto the metal oxide surfaces have been confirmed by the combination of microscopic and spectroscopic investigations including scanning electron microscopy (SEM), X-ray photoelectron spectroscopy (XPS), and solid-state nuclear magnetic resonance spectroscopy (ss-NMR) that were used to follow the process and to compare with the traditional liquid-phase modification schemes. Vienna Ab Initio Simulation Package (VASP) calculations were used to explore the reaction mechanism and key intermediates.

**SS-TuP-6 XPS Study of the Gas Cluster Ion Beam Sputtering of PTFE and Oxygen-treated PTFE**, *Bing Luo,* University of Minnesota

The XPS depth profiling results of polytetrafluoroethylene (PTFE) and oxygen-treated PTFE using monoatomic argon sputtering and gas cluster ion beam (GCIB) sputtering are reported. We evaluated the degrees of surface damage using these two sputtering methods. We found a mild surface damage under GCIB sputtering. On the non-sputtered PTFE surface, only $CF_2$ was present. After GCIB sputtering, $CF_3$ and CF groups were detected. Consistent with the results in the literature, monoatomic Ar sputtering induced a higher degree of damage; the $CF_3$ and CF levels were much higher than those obtained in the GCIB sputtering. The GCIB sputtering of the oxygen-treated PTFE samples revealed that the oxidation layer was mainly located in the top 10 nm. Below 10 nm, the oxygen content became insignificant. Analyzing the distribution of various carbon-fluorine species and comparing to the untreated samples indicated that in the layer from 10 to 60 nm, the PTFE composition or structure was altered by the oxygen treatment, and even at the depth of 120 nm, the property of the PTFE was affected by the oxygen treatment.

**SS-TuP-7 Ultra-high Resolution Imaging of Polymers using Atomic Force Microscopy: Structure and Property at Nanoscale**, *V Korolkov,* Oxford Instruments-Asylum Research*; A Summerfield,* University of Manchester, UK*; A Murphy, D Amabilino,* University of Nottingham, UK*; P Beton,* The University of Nottingham, UK*; M Kocun,* **Roger Proksch,** Oxford Instruments-Asylum Research

Polymers, both synthetic and natural, are ubiquitous materials whose properties are strongly influenced by packing, conformation, and monomer composition of individual macromolecules. The ability to acquire real-space images of the microstructure of these materials with molecular-scale resolution is required to advance the understanding and control of their local ordering, a key element in the precise engineering of polymer properties. Real-space images of polymers with sub-molecular resolution could provide valuable insights into the relationship between morphology and functionality of polymers, but their acquisition is problematic due to perceived limitations in atomic force microscopy (AFM).

Here we show that individual polymer chains and sub-molecular resolution may be achieved using AFM under ambient conditions through the low-amplitude ($\leq$ 1 nm) excitation of higher eigenmodes[1] of a cantilever on a range of commercial polymers (polythiophenes (PTs), polytetrafluoroethylene (PTFE), polyethylene(PE)). We have used this new approach to characterize both single strands of polymers adsorbed on surfaces as well as bulk semi-crystalline samples with Angstrom resolution. For example, on the surface of a spin-coated PT thin film, in which the thiophene groups are perpendicular to the interface, we resolve terminal CH3-groups in a square arrangement with a lattice constant 5.5A from which we can identify abrupt boundaries and also regions with more slowly varying disorder, which allow comparison with proposed models of PT domains. At the same time, bimodal tapping or AM-FM imaging[2] enables modulus mapping on a wide range of polymer materials. Furthermore, molecular-level spatial resolution was achieved with AM-FM imaging on polymer chains in ambient conditions and revealed chain spacing and conformation predicted by theory and other experimental methods.

Our results highlight the important role for high-resolution AFM in determining the properties of polymer strands and thin films of technological relevance, and we anticipate future progress in correlating device performance with structural properties at the sub-molecular scale based on this technique.

[1]Korolkov et al., Nat. Comm., 2019

[2]Kocun et al., ACS Nano, 2017

**SS-TuP-9 Determining the Surface Electrical Potential at the Air/Water Interface**, *Tehseen Adel,* S Baumler, H Allen, The Ohio State University
Several biological and chemical processes directly relate to the organization of molecules at the liquid surface. The surface electric potential across the air/liquid interface provides insight into the molecular organization and propagation of electrical fields by these surface molecules. Using a homemade Air Ionizing Surface Electrical Potential instrument, we measure the surface electrical potential of water, several pure solvents, and inorganic electrolyte solutions without disruption to the liquid surface. Alpha particle radiation from an ionizing source reduces the resistivity of the air gap above the liquid sample, establishing a closed electrical circuit for voltage measurements. From the measured surface potential, we show (i) the orientation of interfacial solvent molecules in pure solvents, and (ii) ascertain the propensity of specific aqueous ions with respect to the air/solution boundary.

**SS-TuP-10 Surface Photovoltage Studies of UV-driven Hydrophilic Flipping in Polysulfone Thin Films**, *John Reeks, N Posinski,* Texas Christian University*; T Haun,* Home School High School Student*; H Hilton,* Texas Christian University*; A Dorward,* Washington and Lee University*; E Bormashenko,* Ariel University, Israel*; Y Strzhemechny,* Texas Christian University

It has been shown in previous studies that hydrophobic surfaces of polysulfone flip to become hydrophilic upon exposure to UV radiation. The exact mechanisms driving this phenomenon are not completely understood. We suggest that elucidation of the surface charge transport phenomena of the as-deposited and UV-irradiated polysulfone could explicate the conversion mechanism and thus contribute to the improved applications of polysulfone on the micro- and nanoscale for novel applications in microfluidics and biophysics. To investigate the UV-driven hydrophilic flipping we performed surface photovoltage (SPV) studies on thin polysulfone films spin-cast on silicon substrates. Since SPV is sensitive to buried interfaces, the resulting spectra are expected to be comprised of features originating not only from the polysulfone films, but also from the silicon wafer and the silicon oxide layer beneath the polymer films. Thereby, to identify the signal germane to polysulfone proper, we employed in our studies polysulfone films of varying and controllable thicknesses to be probed with SPV spectroscopy as well as SPV transient experiments. SPV measurements on Si substrates acted as a control for comparison. Our experiments revealed that SPV yield is significantly affected by the polysulfone films. In particular, we observed significant polarity reversal in the SPV transients in the samples with polysulfone films, whereas SPV spectra indicated transitions at 1.1-1.5 eV appearing in the polysulfone layers. We also report on the comparison of the SPV response in the as-deposited and UV-irradiated polysulfone samples.

**SS-TuP-11 Tuning Spontaneous Supramolecular Assembly *via* Manipulation of Intermolecular Forces and Growth Environment**, *Ryan Brown,* Clarkson University
This poster will detail the initial experiments attempting to exploit non-equilibrium growth conditions to manipulate the spontaneous assembly of functionalized porphyrin molecules at the solid interface. Rapid evaporation of a solution can be considered a non-equilibrium growth environment, one in which a supersaturated thin film is produced and which can result in the formation of metastable supramolecular structures. Our research program seeks to manipulate the frequency and nature of the metastable structures produced in this process by varying the chemical functional groups on a porphyrin ring (and thus intermolecular interactions), the solid substrate (and thus molecule-substrate interactions), and the deposition conditions (varying the rpm and solvent during spin coating deposition). This research is achieved by imaging molecule-decorated surfaces with scanning tunneling microscopy to locally probe the supramolecular structures produced under a given deposition condition. Structural models are then confirmed using electronic structure theory and then applied to understand how the combination of intermolecular forces, molecule-substrate interactions, and conditions in the evaporating solvent influence spontaneous assembly behavior.

**SS-TuP-12 State-Resolved Dissociative Chemisorption Dynamics with RAIRS Product Detection**, *Laurin Joseph,* S Shepardson-Fungairino, A Utz, Tufts University

State-Resolved Dissociative Chemisorption Dynamics with RAIRS Product Detection

Laurin Joseph, Sally Shepardson-Fungairino, and Arthur Utz

State-resolved molecular beam molecular beam experiments use energy and quantum-state selected reactants to understand how specific molecular motions (molecular vibration, rotation, and translation) promote transition state access and chemical reactivity. They also generate experimental data that serve as rigorous benchmarks for DFT-based predictions of reaction barriers and dynamics.

We are currently updating one of our differentially pumped molecular beam reaction chambers to incorporate Reflection Absorption Infrared Spectroscopy (RAIRS) detection of surface-bound reaction products. This capability will allow for real-time, coverage-dependent studies of the reactions occurring on metal surfaces, will provide structural fingerprints of reaction products, and will open the door to the study of larger, more chemically complex, reactant molecules. This poster will survey our progress to date and present preliminary reactivity data for methanol dissociation on a Ru(0001) surface.

**SS-TuP-13 The Two-faced Role of Steps in the Isotopic Scrambling of Hydrogen on Pt**, *Richard van Lent,* L Juurlink, Leiden University, Netherlands
The simplest heterogeneously catalyzed reaction possible is isotopic scrambling of hydrogen:

$H_2 + D_2 \rightarrow 2\,HD$
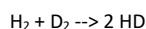
On Pt, this reaction occurs by dissociative adsorption of $H_2$ and $D_2$, mixing of H and D atoms on the surface, and recombination to form the three isotopologues, $H_2$, $D_2$, and HD. Full isotopic scrambling would lead to a product ratio of 1:1:2.

Step edges are well-known to enhance dissociative adsorption, especially at low impact energies. However, it is unknown whether subsequent diffusion and desorption only occur along the steps or involves diffusion onto terraces. We study this by combining supersonic molecular beam techniques with a curved Pt single crystal surface with straight A and B type step edges, c-Pt(111)[1-10]31⁰. At a high surface temperature, we probe HD formation, spatially resolved, along the curved surface by impinging a

50:50 mixture of low energy $H_2$ and $D_2$. HD formation tracks the trend in dissociation: higher step densities yield higher HD formation. However, relatively, HD formation does not increase as rapidly as the dissociation probability. We explain why the (111) terraces are more selective toward HD formation and show that anisotropic diffusion affects isotopic scrambling.

### SS-TuP-14 It's Not just the Defects - How Terrace Symmetry Impacts $H_2O$ Adsorption at Ag Step Edges, S Auras, *Ludo Juurlink,* Leiden University, Netherlands

We investigate water desorption from hydrophobic surfaces using two curved Ag single crystals centered at (111) and (001) apices. On these types of crystals the step density gradually increases along the curvature, allowing us to probe large ranges of surface structures in between the (001), (111) and (110) planes. Subtle differences in desorption of submonolayer water coverages point toward structure dependencies in water cluster nucleation. The B-type step on hydrophobic Ag binds water structures more strongly than adjacent (111) planes, causing preferred nucleation at steps. This driving force for step-induced nucleation is smaller for A-type steps on(111) terraces. The A'-type step flanked by (001) terraces shows no indication of preferred adsorption to steps. Extrapolation to the (311) surface, not contained within either curved surface, demonstrates that both A- and A'-type steps can be regarded chemically identical for water desorption. The different trends in desorption temperature on the two crystals can thus be attributed to stronger water adsorption at (001) planes than at (111) planes and identical to adsorption at the step. These results show that our approach to studying the structure dependence of water desorption is sensitive to variations in desorption energy smaller than 'chemical accuracy', i.e.1 kcal/mol.

### SS-TuP-15 Hydration Lubrication Between Hydrophobic and Hydrophilic Surfaces, *Nir Kampf,* I Rosenhek-Goldian, W Lin, J Klein, Weizmann Institute of Science, Israel

How water rearrange above large stable, smooth, highly hydrophobic surface? We addressed this question by directly measure normal forces and sliding friction under aqueous environment between a negatively-charged hydrophilic mica surface and a fluoropolymer (AF) hydrophobic film, using a surface force balance. The roughness of the AF film was 0.3 nm determined under water by AFM. Normal-force vs. surface-separation profiles indicate that the hydrophobic surface is highly negatively-charge, in line with previous studies and attributed to adsorbed –OH⁻ ions. Sliding of the compressed surfaces under water or salt solution reveals remarkably low friction (friction coefficient $\mu \approx 0.003 - 0.009$) up to applied pressures of at least 50 atm. Hydration lubrication by trapped hydrated counterions between the surfaces is well explained this efficient lubrication, exist in systems like artificial implants, contact lenses, etc. Moreover, molecules that are present in the biological systems were found to adsorb on the charged hydrophobic surface, contributing to reduced friction.

Reference:

Irit Rosenhek-Goldian*; Nir Kampf*; Jacob Klein (2018). Trapped Aqueous Films Lubricate Highly Hydrophobic Surfaces. ACS Nano. 12:(10)10075-10083.

*equally contributors

### SS-TuP-17 Common Errors in XPS Peak Fitting, *George H. Major,* Brigham Young University; *C Easton,* CSIRO Manufacturing; *W Skinner,* Future Industries Institute; *D Baer,* Pacific Northwest National Laboratory; *M Linford,* Brigham Young University

X-ray photoelectron spectroscopy (XPS) is the most popular method for chemically analyzing surfaces, being used in many areas of research and technology. XPS spectra have layers of information that can be extracted with proper analysis. Information ranges from a basic understanding of components (elements) present in a material to advanced peak fitting and background analysis that reveal chemical states and sample morphologies. There are many examples of good XPS peak fitting in the scientific literature. However, the process of peak fitting XPS spectra is still a mixture of art and science and in many cases have no absolutely correct fits. The peak fitting process can be affected by the instrument design and components, experimental settings, and the sample. Here, we discuss a series of common errors that regularly appear in XPS peak fitting in the literature and how to avoid them. These include: (i) not plotting the data according to the international convention with binding energy increasing to the left, (ii) presenting and interpreting data that are far too noisy to be interpretable, (iii) labeling noise as chemical components, (iv) not showing

the original data -- only showing the synthetic (fit) peaks and their sum, (v) not showing any background in a fit, (vi) not providing the sum of the fit components, which makes it difficult for the future reader to determine the quality of a fit, (vii) having widely varying peak widths in a fit, e.g., using extremely broad and extremely narrow peaks when there is no chemical reason for doing so, (viii) having a baseline completely miss the noise/background on either side of the peak, (ix) not collecting data over a wide enough energy window to see a reasonable amount of baseline on both sides of the peak envelope, i.e., truncating the peak, (x) in a fit to a C 1s spectrum, reversing the labeling of the C-O and C=O fit components, and other mislabeling of the components in this envelope (fitting the C 1s peak envelope is well understood so these types of errors should not be made), (xi) for the most part, higher oxidation states of elements correlate with higher binding energies; unfortunately, fit components at higher binding energies are sometimes incorrectly labeled as coming from lower oxidation states, (xii) not taking spin-orbit splitting into account when it is necessary, and/or using inappropriate ratios for these pairs of peaks, and (xiii) in a comparison of related spectra, employing widely different peak widths and positions for components that are supposed to represent the same chemical state and/or using different background types or obviously different types of synthetic peaks in these spectra.

### SS-TuP-18 Exploring the Extent of Hydrogen/Deuterium Exchange on Au(111) between Molecularly-bound Surface Species, *Hasan Kaleem,* E Maxwell, M DePonte, J Baker, M Gillum, D Boyle, A Baber, James Madison University

The exchange between hydrogen and deuterium atoms in molecularly-bound surface species can occur at low temperatures on Au(111). The hypothesized mechanism for the hydrogen/deuterium exchange in ethanol-OD and water is by the Grotthuss mechanism facilitated by hydrogen-bonded molecular networks on Au(111). Therefore, the molecular orientation and packing is central to this exchange. In an effort to rationalize the hypothesized mechanism and realize the extent of hydrogen/deuterium exchange at low temperatures, the co–adsorption of fully deuterated ethanol ($EtOD_6$) and water were investigated. The fragmentation pattern for $EtOD_6$ was first monitored using temperature programmed desorption (TPD), before increasing amounts of water were added to Au(111). A broad range of masses distinct to $EtOD_6$ were monitored using a mass spectrometer and desorption areas were quantified from TPD spectra. Comparing fractional coverages for hydrogen-exchanged $EtOD_6$ products suggest that hydrogen/deuterium exchange predominantly occurs through the hydrogen-bonded network.

### SS-TuP-19 First–Principles Study of on-surface and Sub-surface Oxygen in Rh(111), *Kate Fanning,* W Walkosz, Lake Forest College; *J Garcia, H Iddir,* Argonne National Laboratory; *D Killelea,* Loyola University Chicago

The interaction of oxygen with metal surfaces can directly alter their properties. On-surface and sub-surface O was shown to be a precursor for oxide formation and greatly affect the reactivity of catalytic surfaces [1-4]. Using Density Functional Theory calculations, we investigate various structures of O on the (111) surface of Rh as well as the competition between oxide formation and dissolution of oxygen into Rh to form subsurface oxygen. In particular, the work focuses on identifying pathways for surface diffusion of low-coverage adsorbed atomic O between different sites on Rh(111) as well as the surface to subsurface diffusion. The obtained results are expected to further our understanding of the chemistry of transition metal surfaces.

[1] Rose, M. K.; Borg, A.; Mitsui, T.; Ogletree, D. F.; Salmeron, M. J. Chem. Phys. 2001, 115, 10927-10934.

[2] Monine, M.; Pismen, L.; Bar, M.; Or-Guil, M. J. Chem. Phys. 2002, 117, 4473-4478.

[3] Xu, Y.; Greeley, J.; Mavrikakis, M. J. Am. Chem. Soc. 2005, 127, 12823-12827.

[4] Rotermund, H. H.; Pollmann, M.; Kevrekidis, I. G.Chaos 2002, 12, 157-163.

### SS-TuP-20 STM/S Study of Domain Walls and Atomic Defects on the Surface of Iron-based Superconductors, *Zhuozhi Ge,* Q Zou, M Fu, L Sanjeewa, A Sefat, Z Gai, Oak Ridge National Laboratory

Surface defects, including domain walls and individual atomic defects, can dramatically modify the properties of iron-based superconductors.

However, the nature of domain walls and atomic defects on the surface of in-situ cleaved iron-based superconductors has yet to be identified. Here, we systematically investigated the surface defects on low-temperature cleaved parent and doped $BaFe_2As_2$ superconductors by scanning tunneling microscopy/spectroscopy (STM/S). STM imaging reveals two types of domain walls on parent and Ni/Co doped $BaFe_2As_2$, one as dark trench with missing atoms and the other as straightly aligned bright blobs. Two types of point defects are also identified, one intrinsically from growth or cleaving and the other induced by scanning of the STM tip. Tunneling spectroscopy shows similar surface states at about -200 meV on domain walls and the intrinsic point defects, while on the tip-induced defects there is only one peak at about -120meV.

# Author Index

## Bold page numbers indicate presenter